International Journal of Chemical, Materials and Biomolecular Sciences
ISSN: 2415-6620
Vol:5, No:7, 2011

Residence Time Distribution in a Two Impinging Streams Cyclone Reactor: CFD Prediction and Experimental Validation

Nahid Ghasemi[a], Morteza Sohrabi[b] and Yasan Soleymani[c]

***Abstract*—**The quantified residence time distribution (RTD) provides a numerical characterization of mixing in a reactor, thus allowing the process engineer to better understand mixing performance of the reactor.This paper discusses computational studies to investigate flow patterns in a two impinging streams cyclone reactor(TISCR) . Flow in the reactor was modeled with computational fluid dynamics (CFD). Utilizing the Eulerian-Lagrangian approach, implemented in FLUENT (V6.3.22), particle trajectories were obtained by solving the particle force balance equations. From simulation results obtained at different Δts, the mean residence time (t_m) and the mean square deviation (σ^2) were calculated. a good agreement can be observed between predicted and experimental data. Simulation results indicate that the behavior of complex reactor systems can be predicted using the CFD technique with minimum data requirement for validation.

***Keywords*—**Impinging streams reactor, Residence time distribution, CFD, Eulerian-Lagrangian approach

I.Introduction

One of the most important operations in chemical engineering is the mass transfer between immiscible phases. In impinging streams apparatus a unique flow behaviour is utilized by which the transfer processes in heterogeneous systems are intensified. Application of the impinging streams systems was first proposed by Elperin in the early (1960s) as a device for intensifying transfer processes[1]. In such systems two feed streams, flowing parallel or counter currently collides with each other at a zone in which the two streams impinge.This phenomenon yields the following effects which intensify the heat and mass transfer in particulate systems.

1. Increase in the relative velocities of the phases.
2. Increase in the residence time of particles due to the oscillatory motion of the latter within the continuous phase.
3. Promoting the effective area for mass and heat transport phenomena that is virtually identical to the total surface of particles in the flow.
4. Perfect mixing within the impinging region which in turn enhances the mass and heat transfer rates [2].

The applications of the TISC reactors in industry require the knowledge of appropriate scale-up rules. Since RTD is one of the major parameters required for design . It is thus a fundamental concept in reactor design. The RTD depends on the flow hydrodynamics and the reactor geometry, it has major influence on the reactor chemical performance criteria such as conversion and yield. Hydrodynamics, residence time distribution (RTD) of particles have been experimentally studied in a impinging streams reactors [3-7]. The viability of computational fluid dynamics (CFD) for the design and optimization of chemical reactors has been demonstrated for a variety of systems [8-10]. With the rapid advancement of computational technology, an increasing numbers of studies on RTD in reactors, using CFD have been published in recent years [11-17], but in the best of our literature search, this is the first one on impinging reactor. It should be noted that some studies have performed on impinging jets reactors[18-24].In this study, the ability of the model to predict the RTD of the solid phase at steady flow, applying Fluent software was tested. The major aims of the present investigation are: (a) to simulate the RTD of solid particles، (b) to determine the variance and mean residence time and، (c) to compare the predicted results with the experimental data.

II.System simulation

The TISCR used in the present study is shown schematically with detailed information concerning its geometric dimensions in Fig.1.

To determine the RTD of particles within the system sands with 2.5 g/cm^3 solid density were used as solid particles and water as the fluid phase . However, the determination of particles RTD normally encounters major difficulty. Consequently, only a small number of tagged particles can be used in tracer experiments in order to avoid disturbing the flow conditions. In the present study, some 200 painted sands were applied as the tracer. The method for measurement of RTD of solid phase has been devised previously by Sohrabi et al [4,25].

Three series of RTD curves were determined by varying Δt (0.182، 0.231 and 0.362 s). The mean residence time (t_m) and the variance of the data (σ^2) were calculated as follows:

A. Islamic Azad University, Arak Branch, Arak، Iran (phone : +98-861-3663041 ; fax: +98-861-3670017; e-mail: N-Ghasemi@iau-arak.ac.ir) .
B. Department of Chemical Engineering ,Amir kabir University of Technology, Tehran, Iran (e-mail: sohrabi@aut.ac.ir).
C. Islamic Azad University ، Arak Branch, Arak، Iran . (e-mail: yasansoleymani@yahoo.com).

$$t_m = \frac{\sum_{i=1}^{n} t_i C_i \Delta t_i}{\sum_{i=1}^{n} C_i \Delta t_i} \quad (1)$$

$$\sigma^2 = \frac{\sum_{i=1}^{n} (t_i - t_m)^2 C_i \Delta t_i}{\sum_{i=1}^{n} C_i \Delta t_i} \quad (2)$$

where, n, is the total number of cells containing tagged particles in the rotating disc, as described by Sohrabi et al[***]. In general, n = ∞, however, in the present study, n = 23; Δt, is the time interval between the two consecutive cells and is a constant value for a certain rotational speed of the disc; C_i is the number of tagged particles in i^{th} cell and $t_i = i\Delta t$.

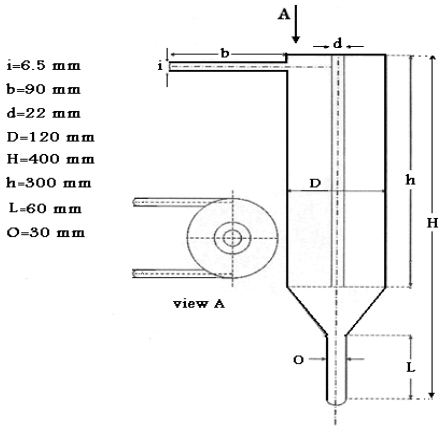

Fig. 1 TISCR applied by sohrabi et al [25]

CFD modeling of an impinging reactor requires complete specification of the flow domain, boundary and initial conditions. Owing to the flow complexity, it is not practical to compare the experimental data obtained for flow domain, with those determined by numerical solution for each individual cell. However, CFD results can be examined by the experimental data available for battery limits. From two injection sources, 200 particles were introduced to the system. This provides a practical method for RTD measurement. To obtain a CFD solution for a General Mixing Problem, mass, momentum and energy balances should be set up and solved.

$$\frac{\partial}{\partial x_i}(\rho u_i) = M_m \quad (3)$$

$$\frac{\partial}{\partial x_i}(\rho u_i u_i) = -\frac{\partial P}{\partial x_j} + \frac{\partial}{\partial x_i}\left[\mu\left(\frac{\partial u_i}{\partial x_j} + \frac{\partial u_j}{\partial x_i}\right) - \rho\overline{u_i u_j}\right] + M_F \quad (4)$$

$$\frac{\partial}{\partial x_i}(\rho c_p u_i T) = \frac{\partial}{\partial x_i}\left[k\frac{\partial T}{\partial x_i} - \rho\overline{u_i T}\right] + M_h + M_l \quad (5)$$

where:

$$\rho\overline{u_i u_j} = \mu_i\left(\frac{\partial u_i}{\partial x_j} + \frac{\partial u_j}{\partial x_i}\right) - \frac{2}{3}\delta_{ij}\frac{\partial u_l}{\partial x_l} \quad (6)$$

$$\rho\overline{u_i T} = \frac{\mu_i}{\sigma_T}\frac{\partial T}{\partial x_i} \quad (7)$$

From Eulerian-Lagrangian approach, the particle's trajectories are obtained by solving the force balance for the latter. The governing equation, by considering the discrete phase inertia, aerodynamic drag, gravity g_{xi} and optional F_{xi}, may be presented as follows:

$$\frac{du_{pi}}{dt} = C_D\frac{18\mu}{\rho_p d_p^2}\frac{\mathrm{Re}}{24}(u_i - u_{pi}) + g_{xi}\frac{\rho_l - \rho}{\rho_l} + F_{xi} \quad (8)$$

where:

$$\mathrm{Re} = \frac{\rho d_p |u_p - u|}{\mu} \quad (9)$$

$$C_D = a_1 + \frac{a_2}{\mathrm{Re}} + \frac{a_3}{\mathrm{Re}^2} \quad (10)$$

If the turbulence model is applied to the solution, the above equation can be used in the turbulent flow regime. In the present work, Standards k-ε model was used to describe the turbulent model in a reliable and optimum computational time. In this model two parameters, namely the turbulent kinetic energy and its dissipation rate are used. This model has been successfully used by a number of researchers.

Standards k-ε model is described as follows:

$$\rho\frac{Dk}{Dt} = \frac{\partial}{\partial x_i}\left(\left(\mu + \frac{\mu_t}{\sigma_k}\right)\frac{\partial k}{\partial x_i}\right) + G_k + G_b - \rho\varepsilon - Y_M \quad (11)$$

Y_M represents the contribution of the fluctuating dilatation in compressible turbulence to the overall dissipation rate, was calculated as follows:

$$Y_M = 2\rho\varepsilon M_t^2 \quad (12)$$

where M_t is the turbulent Mach number.

$$\rho\frac{D}{Dt}(\varepsilon) = \frac{\partial}{\partial x_i}\left(\left(\mu + \frac{\mu_t}{\sigma_\varepsilon}\right)\frac{\partial \varepsilon}{\partial x_i}\right) + C_{1\varepsilon}\frac{\varepsilon}{k}(G_k + C_{3\varepsilon}G_b) - C_{2\varepsilon}\rho\frac{\varepsilon^2}{k} \quad (13)$$

Turbulence constans :

$C_{1\varepsilon}$=1.44 , $C_{2\varepsilon}$=1.92 , $C\mu$ =0.09 , $C_{\sigma k}$=1.0 , $C_{\sigma\varepsilon}$=1.3

A commercial software, GAMBIT 2.3.16 was used to create the 3D flow domain. To ensure grid independency of the results, three meshes (22168, 82222and 192200 cells) have been tested for TISCR. The results indicated that the data for flow velocities were totally independent from the number of cells of the grid. Grid 1 was, therefore, selected for the whole calculations(Fig. 2).

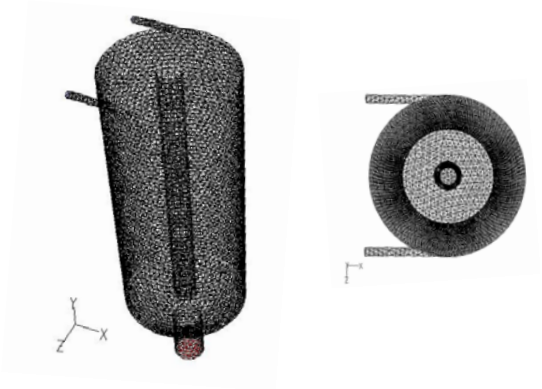

A **B**

Fig. 2 Schematic of the TISCR used in the simulations:(A) Side view and(B) top view

A commercial CFD software package, Fluent (V6.3.22), was applied to solve the conservation of mass and momentum equations for the specified geometries. Water at 293 K was taken as the operating fluid. Inlet velocities, with 10% turbulent intensity, and a uniform velocity distribution were defined and a fully developed flow (outflow) was specified at the exit. In this study, solver was adjusted at steady state, coupled and implicit to solve the governing equations, starting with a first order upwind scheme, and continuing with the second-order upwind scheme for the final converged solution. The SIMPLE method was chosen for the pressure–velocity coupling. The common method for accepting the convergence of the solution is to check and monitor the residuals. Thus, convergence of the numerical solution was censured by monitoring the scaled residuals of continuity, x, y and z velocities components, and the turbulence parameters to a criterion of less than 10^{-3}.

III. Results and Discussion

Figures 4 to 6 show the characteristics and flow patterns within the reactor. The velocity vectors were plotted on vertical surfaces (Figures. 3-4). As observed, in Fig.5, the crossing surface passes through the reactor's contact zone, and in Fig. 6 , throughout TISCR , the effects of vertical motion and collision are significant in this area..

In Figures 7-11, a comparison has been made between the results obtained from RTD simulation of solid particles and the experimental data determined at different Δts. There are a number of data fluctuations as shown in Fig. 7. This is due to the selection of short time intervals. Such fluctuations are formed from internal vibrations of tracer particles in the contact region and are clear demonstrations of random motions of the latter during small Δts. In addition, the peak in simulated RTD graph appears in cell 3 and that determined from experimental studies in cells 1.4.

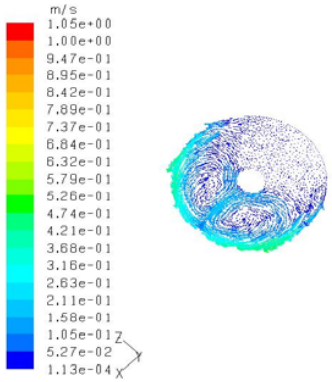

Fig. 3 Computed velocity vectors plotted in contact zone (y=0.29 cm)

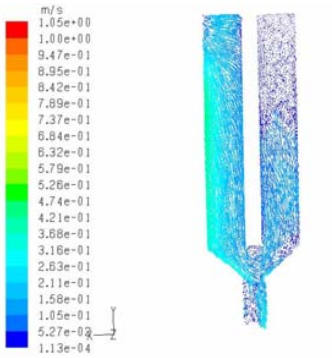

Fig.4 The velocity vectors are plotted on horizontal surface passing through the reactor (z=0 cm)

Fig.8, depicts the results, at Δt=0.231 (s). In this figure it may be observed that some of the data fluctuations are decreased. In addition, the peak determined from simulation is shown in cell 2.2 and that for experimental RTD in cell 1. As it is shown in this figure, the first few cells have received larger portions of the total number of tracer. This may indicate that a large portion of the entering materials to the reactor has very short residence times.The data fluctuations in Fig.9 when each cell has spent 0.362 seconds under the exit port are not observable. This is because at larger Δts, the effect of random motions of particles at the contact region of the exit port is terminated. The peak determined from simulation is appeared in the cell 1.4 and that from experimental RTD in cell 0.6 .

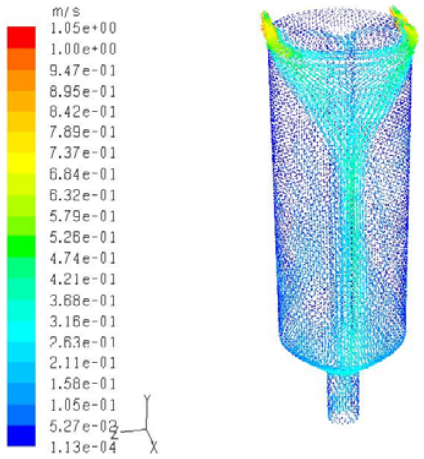

Fig. 5 Computed velocity vectors throughout TISCR

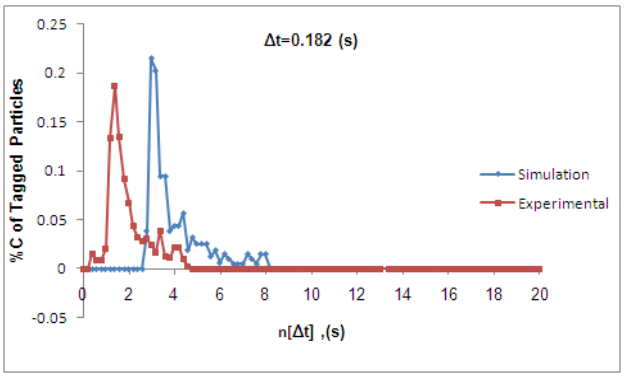

Fig. 6 Comparison between the experimental and simulated RTD data in the TISCR at Δt = 0.182 (s)

As it may be observed from all figures, the peaks in experimental RTD graphs are appeared earlier than those determined from simulation (about 0.3 s). This could be related to both, the errors involved in experimental sampling and the formation of dead regions within the reactor due to the effect of vertical motion. Such a deviation is designated as the transport lag (TL)، a term which is common to both RTD literature and control technology. In other words، TL is equivalent to the number of empty cells in the rotating disc[19]. The simulation and experimental data obtained for different Δt are listed in Table 1.

IV. Conclusion

The CFD method can be used as a proper tool for simulation

TABLE I
DEPENDENCY OF T_M AND Σ^2 ON ΔT

t_m (s)		σ^2 (s^2)		Δt (s)
Simulation	**Experiment**	**Simulation**	**Experiment**	
3.3	1.798	0.55	0.635	0.182
3.6	2.213	1.35	1.366	0.231
3.63	2.291	1.44	1.458	0.362

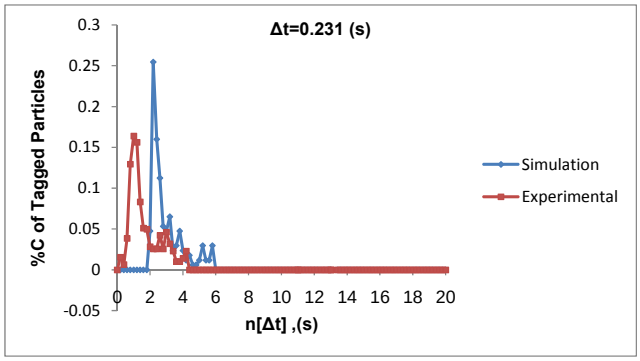

Fig. 7 Comparison between the experimental and simulated RTD data in the TISCR at Δt =0.231 (s)

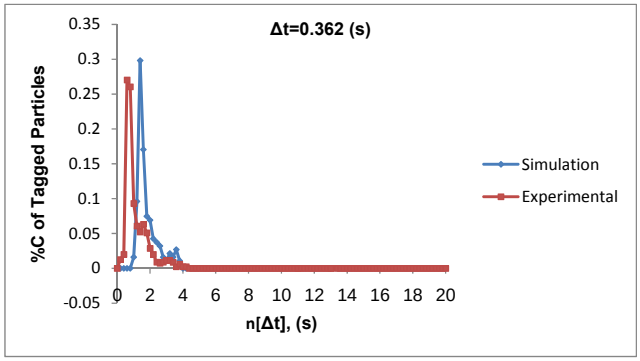

Fig. 8 Comparison between the experimental and simulated RTD data in the TISCR at Δt = 0.362 (s)

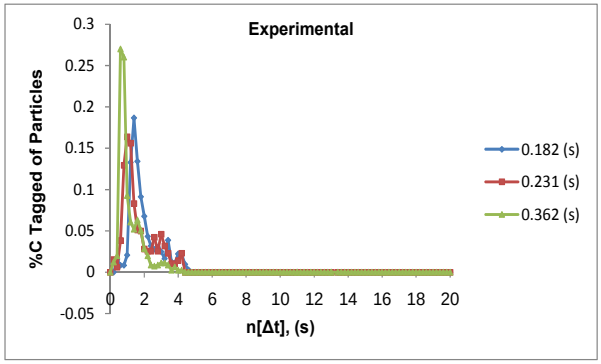

Fig. 9 Comparison between the experimental RTDs in the TISCR at Δt = 0.182, 0.231 and 0.362(s)

and optimization of the processes carried out in TISCR. In prediction of RTD data for a two impinging streams cyclone reactor, it was observed that at a time increment Δt=0.231 and

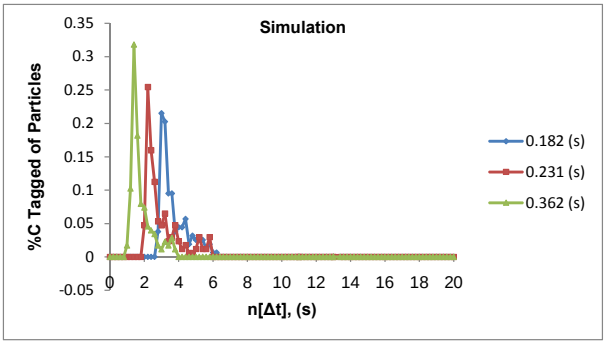

Fig. 10 Comparison between the simulated RTDs in the TISCR at Δt = 0.182, 0.231 and 0.362 (s)

Δt=0.362 s, a close correlation was found between the experimental results and those calculated by CFD technique with a mean absolute deviation of *ca* 1%. The determination of reacting systems behaviors by experimental studies is normally time consuming processes. In addition, design and construction of experimental equipments and preparation of chemicals are usually difficult and impose high expenses. On the other hand, by application of CFD technique the behavior of complicated systems may be readily predicted with the minimum data requirement.

NOTATION

a	Model constants	
c	Model constants	
C_D	Drag coefficient	
C_p	Heat capacity	$J\ kg^{-1}K^{-1}$
d_p	Droplet dimater	μm
G	Generation of turbulence kinetic energy	
k	Turbulent kinetic energy	$m^2\ s^{-2}$
M	Source term in N-S equation	
P	Pressure	Pa
T	Temperature	K
U	Velocity	$m\ s^{-1}$
Y_M	Contribution of the fluctuating dilatation	

Greek Symbols

ε	Energy dissipation rate	$m^2\ s^{-3}$
$\sigma_{\varepsilon,k}$	Model constants	
ρ	Density	$Kg\ m^{-3}$
μ	Viscosity	$N\ s\ m^{-2}$
μ_t	Turbulent viscosity	$N\ s\ m^{-2}$

Subscripts

l	Liquid
p	Particle
K	Kinetic energy
B	buoyancy

REFERENCES

[1] I. Elperin, Heat and Mass Transfer in Impinging Streams, Inzh. Fiz. Zh. 6 ,1961, pp. 62-68.
[2] S. J. Royaee, M. Sohrabi, Application of photo-impinging streams reactor in degradation of phenol in aqueous phase,Desalination. 253 ,2010, pp. 57–61.
[3] M. Sohrabi, B. Zareikar, Modeling of the residence time distribution and application of the continuous two impinging streams reactor in liquid–liquid reactions, Chem. Eng. Technol. 28 ,2005, pp. 61-66.
[4] M. Sohrabi, I. Sepahsalari, Studies on the hydrodynamic behaviour and modeling of the residence time distribution in a coaxial flow two impinging streams cyclone reactor, Afinidad, 2005, pp. 62, 307.
[5] Y. Kitron, A. Tamir, Performance of a coaxial gas-solid two-impinging streams (TIS) reactor: hydrodynamics, residence time distribution, and drying heat transfer، Industrial and Engineering Chemistry Research، 27,1989, pp. 1760–1767.
[6] A. Tamir, M. Grinholtz, Performance of a continuous solid–liquid two impinging streams (TIS) reactor: dissolution of solids, hydrodynamics, mean residence time and holdup of the particles، Industrial and Engineering Chemistry Research، 26, 1998, pp.726–731.
[7] M. Sohrabi, M. Ahmadi Marvast, Measurement of holdup and residence time distribution in a two impinging streams cyclone reactor, J. Chin. Inst. Chem. Engrs, 33, 2002, pp. 167.
[8] D.L. Marchisio, A.A. Barresi, CFD simulation of mixing and reaction: the relevance of the micro-mixing model, Chem. Eng. Sci. 58, 2003, pp. 3579-3587.
[9] D.A. Sozzi, F. Taghipour, Computational and experimental study of annular photo-reactor hydrodynamics ،Int. J. Heat and Fluid Flow. 27 ,2006, pp. 1043-1053.
[10] L. Hjertager, B.H. Hjertager, T. Solberg, CFD modelling of fast chemical reactions in turbulent liquid flows, Comput. Chem. Eng. 26 ,2002, pp. 507-515.

[11] V.V. Ranade, Computational Flow Modeling for Chemical Reactor Engineering, Academic Press, New York. ,2002.
[12] S. Vedantam, J.B. Joshi, S.B. Koganti, CFD simulation of RTD and mixing in the annular region of a Taylor-Couette contactor، Ind. Eng. Chem. Res. 45 ,2006, pp. 6360-6367.
[13] E.L. Paul, V.A Atiemo Obeng, S.M. Kresta, Handbook of Industrial Mixing: Science and Practice, (Wiley-IEEE) ,2004.
[14] B.S. Choi, B. Wan, S. Philyaw, K. Dhanasekharan, T.A. Ring, Residence time distributions in a stirred tank: comparison of CFD predictions with experiment, Ind. Eng. Chem. Res . 43 ,2004, pp. 6548-6556.
[15] B.S. Choi, B. Wan, S. Philyaw, K. Dhanasekharan and T.A. Ring, Residence time distributions in a stirred tank-comparison of CFD predictions with experiment, In Proceedings of the AIChE Annual Meeting. 2007.
[16] B. Hua , S. Amber, J. Jorge, J. Dennis and G Paul , Modeling flow and residence time distribution in an industrial-scale reactor with a plunging jet inlet and optional agitation، Chem. Eng. Res. 86, 2008, PP. 1462–1476.
[17] F. Ghirelli, S. Hermansson, H. Thunman, B. Leckner، Reactor residence time analysis with CFD, Prog. Comput. Fluid Dynam. 6 ,2006, PP. 241-247.
[18] J.C. Roy, C. Bertrand, and G.L. Palec, Numerical and Experimental Study of Mixed and Forced Convection in a Junction, International Journal of Heat and Mass Transfer, 37, 1994, PP. 1985-2006.
[19] S.M. Hosseinalipour, A.S. Mujumdar, Flow and Thermal Characteristics of Steady Two Dimensional Confined Laminar Opposing Jets: Part I. Equal Jets, International Communications in Heat and Mass Transfer, 24, 1997a, pp. 27-38.
[20] S.M. Hosseinalipour, A.S. Mujumdar, Flow and Thermal Characteristics of Steady Two Dimensional Confined Laminar Opposing Jets: Part II. Unequal Jets, International Communications in Heat and Mass Transfer, 24, (1997b, pp. 39-50).
[21] S.J. Wang, S. Devahastin, and A.S. Mujumdar, Effect of temperature difference on flow and mixing characteristics of laminar confined opposing jets, Applied Thermal Engineering, 26, 2006, pp.519-529 .
[22] S. Devahastin, A.S.Mujumdar, A Numerical Study of Flow and Mixing Characteristics of Laminar Confined Impinging Streams, Chemical Engineering Journal, 85, 2002, pp. 215-223.
[23] S.J. Wang, S.Devahastin, and A.S. Mujumdar, Effects of Geometry and Operating Conditions on the Mixing Behavior of an In-Line Impinging Stream Mixer, Applied Mathematical Modelling, 25, 2005, pp. 253-269.
[24] R.J. Santos et al ,Validation of a 2D CFD Model for Hydrodynamics' Studies in CIJ Mixers, International Journal of Chemical Reactor Engineering ,8 (2010)A32.
[25] M. Sohrabi, S. Fathi Pirkashani, M. Sohrabi, S. Fathi Pirkashani, Application of a tangential flow two colliding streams cyclone reactor in solid-liquid reactions, International Journal of Chemical Reactor Engineering. 5 ,2007, A88.